HHS Public Access

Author manuscript

Neuroimage. Author manuscript; available in PMC 2022 June 01.

Published in final edited form as:

Neuroimage. 2022 June ; 253: 119094. doi:10.1016/j.neuroimage.2022.119094.

Longitudinal changes in the neural oscillatory dynamics underlying abstract reasoning in children and adolescents

Brittany K. Taylor[a,b,*], **Elizabeth Heinrichs-Graham**[a,b], **Jacob A. Eastman**[a], **Michaela R. Frenzel**[a], **Yu-Ping Wang**[c], **Vince D. Calhoun**[d,e], **Julia M. Stephen**[e], **Tony W. Wilson**[a,b]

[a]Institute for Human Neuroscience, Boys Town National Research Hospital, 378 Bucher Circle, Boys Town, NE 68010, USA

[b]Department of Pharmacology and Neuroscience, Creighton University, Omaha, NE, USA

[c]Department of Biomedical Engineering, Tulane University, New Orleans, LA, USA

[d]Tri-institutional Center for Translational Research in Neuroimaging and Data Science (TReNDS), Georgia State University, Georgia Institute of Technology, Emory University, Atlanta, GA, USA

[e]Mind Research Network, Albuquerque, NM, USA

Abstract

Fluid reasoning is the ability to problem solve in the absence of prior knowledge and is commonly conceptualized as “non-verbal” intelligence. Importantly, fluid reasoning abilities rapidly develop throughout childhood and adolescence. Although numerous studies have characterized the neural underpinnings of fluid reasoning in adults, there is a paucity of research detailing the developmental trajectory of this neural processing. Herein, we examine longitudinal changes in the neural oscillatory dynamics underlying fluid intelligence in a sample of typically developing youths. A total of 34 participants age 10 to 16 years-old completed an abstract reasoning task during magnetoencephalography (MEG) on two occasions set one year apart. We found robust longitudinal optimization in theta, beta, and gamma oscillatory activity across years of the study across a distributed network commonly implicated in fluid reasoning abilities. More specifically, activity tended to decrease longitudinally in additional, compensatory areas such as the right lateral prefrontal cortex and increase in areas commonly utilized in mature adult samples

[*]Corresponding author at: Institute for Human Neuroscience, Boys Town National Research Hospital, 378 Bucher Circle, Boys Town, NE 68010, USA. Brittany.Taylor@boystown.org (B.K. Taylor).

Declaration of Competing Interest

All authors report no biomedical financial interests or potential conflicts of interest.

Credit authorship contribution statement

Brittany K. Taylor: Methodology, Validation, Formal analysis, Data curation, Writing – original draft, Writing – review & editing, Visualization. **Elizabeth Heinrichs-Graham:** Conceptualization, Methodology, Investigation, Formal analysis, Writing – review & editing. **Jacob A. Eastman:** Investigation, Data curation. **Michaela R. Frenzel:** Investigation, Data curation, Project administration. **Yu-Ping Wang:** Conceptualization, Funding acquisition. **Vince D. Calhoun:** Conceptualization, Methodology, Investigation, Resources, Data curation, Writing – review & editing, Supervision, Project administration, Funding acquisition. **Julia M. Stephen:** Conceptualization, Methodology, Investigation, Resources, Data curation, Writing – review & editing, Supervision, Project administration, Funding acquisition. **Tony W. Wilson:** Conceptualization, Methodology, Investigation, Resources, Data curation, Writing – review & editing, Supervision, Project administration, Funding acquisition.

Supplementary materials

Supplementary material associated with this article can be found, in the online version, at doi:10.1016/j.neuroimage.2022.119094.

(e.g., left frontal and parietal cortices). Importantly, shifts in neural activity were associated with improvements in task performance from one year to the next. Overall, the data suggest a longitudinal shift in performance that is accompanied by a reconfiguration of the functional oscillatory dynamics serving fluid reasoning during this important period of development.

Keywords

Theta; Beta; Gamma; Fluid reasoning; Development

1. Introduction

Fluid reasoning, or the ability to problem solve in the absence of prior situational knowledge, is a form of non-verbal intelligence that undergoes dynamic, rapid development throughout childhood and adolescence. Prior research has linked fluid intelligence abilities to aptitude in a number of other critical cognitive domains including working memory, processing speed, and crystallized (i.e., verbal) intelligence among others (Conway et al., 2002; Crone and Ridderinkhof, 2011; Ferrer et al., 2009; Mcardle et al., 2002). Given its associations with so many other domains of functioning, it is perhaps unsurprising that fluid intelligence is predictive of outcomes across the lifespan such as academic achievement, life expectancy, work performance, and income (Ferrer et al., 2009; Gottfredson and Deary, 2004; Kievit et al., 2018; Mcardle et al., 2002).

Fluid intelligence generally increases throughout childhood and adolescence before plateauing in young adulthood (Mcardle et al., 2002). Importantly, the development of fluid intelligence abilities, including such skills as abstract reasoning, is closely coupled with brain maturation (Bazargani et al., 2014; Ramchandran et al., 2019; Shaw, 2007). Accumulating evidence over the past two decades commonly implicates a distributed frontoparietal network of brain regions serving fluid intelligence processes (Basten et al., 2015; Dumontheil, 2014; Jung and Haier, 2007; Shaw, 2007). A number of studies have specifically implicated left-hemispheric regions in fluid reasoning abilities, with many fMRI studies showing increased activation in left frontoparietal and temporal areas with increasing reasoning abilities (Basten et al., 2015; Hobeika et al., 2016; Perfetti et al., 2009). These areas of the brain are known to follow a protracted path of maturation extending into adulthood. Structurally, frontoparietal areas exhibit significant gray matter pruning during childhood and adolescence resulting in robust decreases in gray matter thickness and volume (Casey et al., 2000; Wierenga et al., 2014). Further, white matter tracts connecting critical frontal and parietal areas undergo a pivotal architectural reorganization during development (Fuhrmann et al., 2019; Simpson-Kent et al., 2020). These structural changes have been linked to longitudinal improvements in fluid reasoning abilities (Estrada et al., 2019; Simpson-Kent et al., 2020; Wendelken et al., 2017, 2016).

Studies examining the neural oscillatory dynamics serving fluid intelligence regularly implicate frontal and parietal cortices, but frequently produce disparate results concerning which oscillatory dynamics are most critically involved in fluid reasoning. Among mature, healthy adults, some researchers have found that theta (4–8 Hz) oscillatory activity is key

(Neubauer et al., 2017; Pahor and Jaušovec, 2014), whereas others suggest that alpha (8–12 Hz; Neubauer and Fink, 2003; Ramos et al., 1993) or even high-frequency gamma (30 Hz+) responses (Santarnecchi et al., 2016, 2013) most crucially support fluid reasoning. Theta activity in frontal and parietal regions has been strongly tied to cognitive control and higher order cognitive abilities (Cavanagh et al., 2012), including several cognitive functions that are closely coupled with fluid reasoning (e.g., working memory, attention; Jensen and Tesche, 2002; Rajan et al., 2018; Sauseng et al., 2005). In general, theta power is shown to increase as a function of task demands and cognitive effort (Cavanagh and Frank, 2014; Wascher et al., 2014). Likewise, alpha activity in these same regions has been closely linked to higher order abilities, though perhaps in a different capacity. Some research suggests that shifts in alpha power may be indicative of neural inhibition (Cohen and Ridderinkhof, 2013; Sadaghiani et al., 2012). By inhibiting certain processes, neural resources can be redirected to processing relevant inputs for achieving the goal-directed behavior at hand. However, changes in alpha power have also been noted in instances of high cognitive demand, suggesting that increases in alpha power may be indicative of cognitive load and mental effort (Koshy et al., 2020; Meyer et al., 2013; Rosen and Reiner, 2017). Gamma activity in frontoparietal regions has been less well characterized. While some studies suggest that early gamma responses may be beneficial in novel problem solving (Cohen and Ridderinkhof, 2013; Rosen and Reiner, 2017), others have suggested that greater gamma power is indicative of inefficiencies in neural processing (Phillips and Takeda, 2009). Regardless, given the strong links between these three oscillatory responses and high order cognitive abilities, it is perhaps unsurprising that these have been at the center of studies examining the neural dynamics serving fluid reasoning.

Despite the mixed oscillatory results surrounding fluid reasoning abilities, there is a common theme that emerges; basically, greater recruitment of left frontal and parietal areas tends to be associated with a more mature adult-like response, higher overall fluid intelligence, and overall better performance in fluid reasoning tasks among adults. Of course, the neural oscillatory dynamics underlying fluid intelligence abilities also undergo major developmental changes, in line with the robust maturation observed in both behavior and in brain structure during childhood and adolescence. That said, studies examining the developmental trajectory of these neural dynamics are decidedly rare.

One recent study by Taylor et al. (2020) mapped the developmental trajectory of multi-spectral neural oscillatory dynamics serving abstract reasoning abilities in a cohort of children and adolescents. The authors found robust age-related changes specifically in theta (4–8 Hz) oscillatory activity across a distributed frontoparietal network. Importantly, the findings suggested that shifts in theta power as a function of age, particularly in left frontal and parietal regions, supported better behavioral performance during the abstract reasoning task. Another study in a narrow age-range of older adolescents found that alpha (8–12 Hz) oscillations critically index fluid abilities during an analogical reasoning task (Dix et al., 2016). Specifically, larger alpha desynchronizations (i.e., band-limited power decreases) during the task were associated with greater fluid intelligence abilities, faster learning, and better behavioral performance among youths. The findings from these studies are rather intuitive when considering the functional roles of theta and alpha oscillatory activity in the noted brain regions. Namely, theta and alpha activity in left frontoparietal areas has been

commonly implicated in complex cognitive processing like working memory manipulation and directed attention (Cavanagh and Frank, 2014; McDermott et al., 2016a, 2016b; Meyer et al., 2013; Sauseng et al., 2005; Wilson et al., 2016).

The few developmental studies that have focused on the neural oscillatory dynamics serving fluid reasoning abilities have made major contributions to the field's understanding of maturation in these systems. However, these have been purely cross-sectional works and there is a major need for longitudinal studies detailing within-person changes in the oscillatory dynamics over time as fluid reasoning abilities mature. The field has come to the consensus that longitudinal studies are necessary investments for understanding within-person trajectories of change in cognitive and brain development. Longitudinal works have repeatedly shed light on unique aspects of development that are not captured by cross-sectional designs (Feldstein Ewing et al., 2018; Jernigan et al., 2018; Kievit and Simpson-Kent, 2021).

Herein, we extend our previous work published in Taylor et al. (2020) and quantify within-person changes in the oscillatory dynamics serving fluid reasoning in a sample of children and adolescents. All participants completed two magnetoencephalography (MEG) recordings approximately one year apart and performed the same abstract reasoning task during each session. Using robust source imaging methods, we report changes in the neural dynamics underlying fluid reasoning and link these to shifts in behavioral performance. Based on previous works in children (Dix et al., 2016; Taylor et al., 2020), we predicted that youths would exhibit reduced recruitment of compensatory regions over time, and increased recruitment of task-relevant regions as indexed by changes in oscillatory power. Given the limited consensus in the literature on key oscillatory bands of interest, we did not make specific hypotheses as to which frequencies would show changes over time. Finally, we expected that these regional changes in oscillatory power would be associated with improvements in performance on the abstract reasoning task (i.e., faster reaction times, increased task accuracy).

2. Methods

2.1. Participants

The sample was comprised of a subset of youths recruited for the Developmental Chronnecto-Genomic Study (Dev-CoG; Stephen et al., 2021), for which children and adolescents were invited to complete neuropsychological testing and neuroimaging annually for three consecutive years. All participants in the present investigation were recruited from the Omaha, Nebraska site. As part of the longitudinal protocol, youth were asked to complete an abstract reasoning task during MEG in the second and third years of the study. Notably, the current study is an extension of the sample reported in Taylor et al. (2020) and included all youths who completed the abstract reasoning task twice. A total of 45 youth (27 male) completed the abstract reasoning task at two separate visits. Youth were between the ages of 9.99 to 15.96 years-old (M = 12.74 years, SD = 1.66) at time 1, with approximately one year between visits (M = 1.01 years, SD = 0.079, range = 0.90 to 1.34 years). Exclusionary criteria included medical conditions affecting CNS function, neurological or psychiatric disorder, history of loss of consciousness, current substance abuse, current use

of any medication known to affect CNS function, and the MEG Laboratory's standard exclusion criteria (e.g., dental braces, metal implants, battery operated implants, and/or any type of ferromagnetic implanted material). Parents of child participants signed informed consent forms, and child participants signed assent forms before proceeding with the study. All procedures were approved by the university's Institutional Review Board.

Of the 45 participants who completed the abstract reasoning task at both time points, data from 11 participants were excluded from all analyses due to poor performance on the task (< 60% correct; $n_{time1} = 1$, $n_{time2} = 2$), technical problems during data acquisition ($n_{time1} = 3$, $n_{time2} = 0$), or excessive MEG artifacts or outliers ($n_{time1} = 3$, $n_{time2} = 2$). Thus, the final sample was comprised of 34 youth (23 male) who were between the ages of 9.99 and 15.41 years-old ($M = 12.87$ years, $SD = 1.59$) when they first completed the abstract reasoning task, with .90 to 1.17 years between visits ($M = 1.00$ years, $SD = 0.063$). Youth who were included in the final sample did not differ from those who were excluded based on age ($t_{(43)} = -0.96$, $p = .341$, d = 0.319), sex ($\chi^2_{(1)} = 1.28$, $p = .257$), IQ ($t_{(33)} = .056$, $p = .955$, d = .021), or fluid intelligence composite scores ($t_{(43)} = 0.51$, $p = .613$, d = 0.182).

2.2. Cognitive assessments

All participants completed the four-scale Wechsler Abbreviated Scale of Intelligence (WASI-II; Wechsler, 2011) approximately one year prior to the first MEG session reported herein (Stephen et al., 2021). A Full-Scale IQ score, a verbal comprehension index (VCI), and a perceptual reasoning index (PRI) were computed for each participant in accordance with the publisher recommendations. Of note, the PRI composite is an index of fluid intelligence. Each composite from the WASI-II is expected to have a mean of 100 in the population, with a standard deviation of 15. Average scores in the present study were generally above average (Full-Scale IQ: $M = 114.16$, $SD = 13.97$; VCI: $M = 114.27$, $SD = 16.99$; PRI: $M = 111.11$, $SD = 13.35$).

2.3. Abstract reasoning task

The abstract reasoning task has been previously described (Taylor et al., 2020). Briefly, youth were presented with a grid of four boxes surrounding a central fixation point, with one of the two bottom boxes highlighted in white. After a duration of 2750 ms (± 250 ms), the four boxes would populate with complex images for a duration of 4000 ms. Participants were instructed to indicate with a button press whether the figure in the highlighted box correctly completed the matrix of complex images (i.e., a match; see Fig. 1). Patterns could be matched on number, color, or orientation. In total, there were 120 trials with equal numbers of pseudo-randomly presented "match" versus "non-match" trials (additional examples are shown in Supplemental Fig. S1). The task took approximately 14 min to complete, with a 30 s break halfway through the paradigm.

2.4. MEG data acquisition

Neuromagnetic data were recorded using an Elekta MEG system with 306 sensors (204 planar gradiometers; Elekta, Helsinki, Finland) within a one-layer magnetically shielded room with active shielding. MEG data were sampled at 1kHz using a bandwidth of .1 to 330 Hz. Recorded data were corrected for head motion per participant and per session, and noise

reduction was applied via signal space separation with a temporal extension (tSSS; Taulu and Simola, 2006; Taulu et al., 2005).

2.5. MEG coregistration and structural MRI processing

At the start of each MEG session, four coils were attached to the participant's head and localized, along with three fiducial points and the scalp surface using a 3-D digitizer (Fastrak 3SF0002, Polhemus Navigator Sciences, Colchester, VT, USA). Participants were then seated and properly positioned within the MEG. An electric current with a unique frequency was fed to each of the coils (e.g., 322 Hz) allowing measurement of the generated magnetic field which could be localized in reference to the MEG sensors throughout the recording session. Because the coil locations were also known in head coordinates, all MEG measurements could be transformed into a common coordinate system. This coordinate system was used to coregister MEG data to each participant's individual structural T1-weighted MRI prior to source reconstruction in BESA MRI (v. 2; BESA GmbH, Gräfelfing, Germany). Structural MRIs were acquired using a Siemens Skyra 3T MRI scanner with a 32-channel head coil and a MP-RAGE sequence with the following parameters: TR = 2400 ms; TE = 1.94 ms; flip angle = 8°; FOV = 256 mm; slice thickness = 1 mm (no gap); voxel size = 1 × 1 × 1 mm. Acquired images were aligned to the anterior and posterior commissure and transformed into standardized space. Finally, 4.0 × 4.0 × 4.0 mm functional images computed during source analysis (i.e., beamforming) were also transformed into standardized space in the same manner as the structural MRI volumes.

2.6. MEG Time-frequency transformation and statistics

To begin, ocular and cardiac artifacts were removed from the raw data using signal space projection (SSP; Uusitalo and Ilmoniemi, 1997). Continuous magnetic timeseries were epoched into 6500 ms segments, spanning from 2500 ms prior to the stimulus pattern onset, to 4000 ms after (i.e., the duration of the target stimulus presentation). Baseline was defined as −1800 ms to −800 ms prior to the stimulus pattern onset to avoid any potential anticipation effects, although no such effects were apparent in the final analyses. Epochs containing large artifacts (e.g., coughing, swallowing, muscle tension) were rejected by using a fixed threshold method based on the distribution of amplitudes and gradients across trials per participant. The highest values were rejected per participant. Importantly, thresholds were determined based on both signal amplitude (M_{time1} = 1263.07 fT, SD = 308.53; M_{time2} = 1231.84 fT, SD = 308.94) and gradient (M_{time1} = 234.55 fT/s, SD = 137.32; M_{time2} = 212.00 fT/s, SD = 101.62) to better account for differences in sensor proximity and head size between individuals. The number of trials included in analyses did not differ across years in the final sample ($t_{(33)} = -0.26$, $p = .80$, d = 0.058; M_{time1} = 91.94 trials, SD = 10.52; M_{time2} = 91.35, SD = 9.93), nor did it correlate with age ($r_{\text{time1}(34)} = -.004$, $p = .98$; $r_{\text{time2}(34)} = -.097$, $p = .59$).

The remaining artifact-free epochs were transformed into the time-frequency domain via complex demodulation at a 2 Hz and 25 ms resolution. The resultant spectral power estimates were averaged across all trials per sensor, thereby generating time-frequency plots of mean spectral density. Sensor-level data were normalized to the mean baseline power (−1800 ms to −800 ms) per participant. Time-frequency windows for source reconstruction

were determined via statistical analysis of the sensor-level data across all trials, participants, and years, and utilized all gradiometers. Our analyses focused on the first 1000 ms post stimulus onset in order to maximize focus on the cognitive aspects of stimulus processing while minimizing the impact of other brain responses (i.e., motor), which were not of interest in this investigation. Statistical analysis of sensor-level data was completed in a two-step process to minimize Type I error. First, we computed two-tailed paired-samples *t*-tests comparing the data to baseline for each time point, with the output spectrograms thresholded at $p < .05$ across all participants. Time-frequency bins which survived the threshold were then clustered with temporally- and/or spectrally-neighboring bins that also survived thresholding, and a cluster value was derived by summing all *t*-values within the resultant cluster. We then applied nonparametric cluster-based permutation testing with 1000 permutations to build a distribution of cluster values and significance levels (Ernst, 2004; Maris and Oostenveld, 2007). The resultant spectrograms were used to determine time-frequency windows containing significant oscillatory events across all participants, which we then reconstructed into source space. Note that these analyses were completed using MEG data from both time 1 and time 2 recordings in order to reduce any session-specific bias.

2.7. MEG source imaging and statistics

Cortical activity was imaged using an extension of the linearly constrained minimum variance vector beamformer (Gross et al., 2001; Hillebrand et al., 2005; Veen et al., 1997). This beamformer uses frequency-specific spatial filters to compute source power for the entire brain volume. Single images were computed from cross-spectral densities using all possible combinations of gradiometers averaged over the specified time-frequency window, and the solution of the forward problem for each location on a grid specified by input voxel space. We computed noise-normalized source power per voxel in each participant, for each year of the study, using passive (i.e., baseline) and active (i.e., task) periods of equal duration and bandwidth (Hillebrand et al., 2005). The resultant images are referred to as pseudo-*t* maps, with units reflecting noise-normalized power differences between active and passive periods per voxel. MEG preprocessing was completed using BESA Research version 7.0.

For each participant, and for each year of the study, normalized differential source power was computed for the statistically-identified time-frequency windows (see “Sensor-Level Results”) at 4.0 × 4.0 × 4.0 mm resolution. Note that youths whose individual maps contained artifactual activity (peak values exceeding 3 times the standard deviation of the entire sample) within a given oscillatory band were excluded from analyses using those maps. A total of 30 youths were included in analyses of theta oscillatory activity, 27 youths were included in beta oscillatory activity analyses, and 31 youths were included in gamma oscillatory analyses. Note that all analyses were attempted with and without listwise exclusion and yielded similar patterns of results, thus we retained a pairwise exclusion approach per oscillatory band to retain statistical power. The final 3D maps of brain activity were averaged separately for time 1 and for time 2 across all participants to identify the neuroanatomical basis of the significant sensor-level oscillatory responses during the task. For further analyses, we utilized the individual-level maps for each year of the study in order to best capture the nature of individual variability in neural oscillatory dynamics. In

an initial set of analyses, we compared the maps derived for each year of the study using paired-samples *t*-tests to decipher any significant longitudinal changes in neural oscillatory power. We next extracted the pseudo-*t* values from the peak voxel of each significant cluster (4.0 × 4.0 × 4.0 mm resolution) to determine the specific response's relationship to task performance (i.e., reaction time and accuracy), and to cognitive assessments (i.e., the PRI composite from the WASI). Of note, we computed these analyses using pseudo-*t* values extracted from the peak and a cluster average of pseudo-*t* values that included the peak and neighboring voxels that shared a side (of the cube) with the peak. These analyses yielded the same conclusions (see Supplemental Fig. S2); thus, we only report the findings using peak voxel values to ensure the best comparability with other MEG studies, as using the peak voxel in such analyses is by far the most common approach. Relationships to task behavior and neuropsychological assessment were conducted in Mplus version 8.1. In a second set of exploratory analyses, we computed individual subtraction maps for each participant to identify differences in oscillatory activity between time 1 and time 2. We then computed whole-brain correlations between the resultant subtraction maps per participant and changes in task performance across both years of the study. All clusters were conservatively thresholded at a significance level of $p < .005$ and corrected for multiple comparisons using a cluster correction criterion requiring a minimum of at least 5 contiguous voxels (i.e., ≥ 320 mm^3).

2.8. Data/code availability statement

The data used in this article are openly available through the COINS framework (https://coins.trendscenter.org/). See dataset COINS:Dev-CoG. Those who wish to use the data can create an account with COINS and complete a data request process for the study, similar to other major open access data repositories.

3. Results

3.1. Demographic and behavioral data

Youth included in the final sample performed the task well and showed significant improvements in accuracy ($t_{(33)} = 2.63$, $p = .013$, d = 0.402; $M_{time1} = 83.48\%$, $SD = 6.98$; $M_{time2} = 86.18\%$, $SD = 6.45$) and reaction time ($t_{(33)} = -2.65$, $p = .012$, d = 0.313; $M_{time1} = 1949.87$ ms, $SD = 314.17$; $M_{time2} = 1853.96$ ms, $SD = 297.69$) across years of the study. Accuracy and reaction time were both relatively reliable across visits, suggesting that those who were better at performing the task one year tended to perform better in the following year (accuracy: $r_{(34)} = .61$, $p < .001$; reaction time: $r_{(34)} = .76$, $p < .001$). Finally, differences in reaction times and differences in accuracy across years were significantly correlated; individuals who responded faster in time 2 relative to time 1 also tended to be more accurate in time 2 relative to time 1 ($r_{(34)} = -.61$, $p < .001$; see Fig. 2).

3.2. Sensor-Level Results

Time-frequency spectrograms indicated three windows of significant oscillatory activity. There was a significant increase in theta activity (i.e., theta synchronization) relative to baseline from 4 to 8 Hz across a distributed array of sensors from 100 to 400 ms. There was also a strong decrease in beta activity (i.e., beta desynchronization) relative to baseline

from 12 to 18 Hz in posterior and central sensors from 400 to 1000 ms. Finally, an increase in gamma activity (i.e., gamma synchronization) relative to baseline from 80 to 94 Hz was observed in posterior sensors from 100 to 1000 ms (see Fig. 3).

3.3. Functional mapping results

Grand-averaged beamformer images for each of the three time-frequency bins are displayed in Fig. 4, separately for each year of the study. Theta increases relative to baseline were strongest in the occipital cortices during both years of the study, with an extended distribution along primarily right frontal and parietal regions. The activity appeared markedly less diffuse in time 2 relative to time 1. In the beta band, there was a robust decrease relative to baseline in occipital and parietal cortices, with a notable cluster in the left superior parietal. These beta oscillations (i.e., decreases in power relative to baseline) appeared more robust at time 2 relative to time 1. Finally, there was a strong increase in gamma activity relative to baseline confined to occipital areas, which appeared to be similar in magnitude and distribution across years of the study.

To examine differences in neural oscillatory activity across years, we conducted paired-samples *t*-tests comparing the functional activation maps from time 2 to those from time 1. There was a statistically significant decrease in theta activity in time 2 relative to time 1 within the right inferior occipital ($t_{(29)} = -3.69$, $p = .001$, d = 0.495) and lateral prefrontal cortices ($t_{(29)} = -3.67$, $p = .001$, d = 0.709). Conversely, there were significantly stronger beta oscillations (i.e., greater decreases in power relative to baseline) in the right parahippocampal gyrus ($t_{(26)} = -5.56$, $p < .001$, d = 0.685), and in the left inferior frontal ($t_{(26)} = -3.44$, $p = .002$, d = 0.836) and superior temporal gyri ($t_{(26)} = -4.51$, $p < .001$, d = 0.994; see Fig. 5 and Table 1).

We extracted pseudo-*t* values at the peak of each identified cluster for each year of the study and computed the difference in oscillatory power between time 2 and time 1. We then examined the extent to which each peak difference was related to general fluid intelligence and to changes in task behavior using three multivariate regression analyses. For task behavior analysis, models were designed such that the differences in pseudo-*t* values at all five identified clusters were simultaneously modeled as predictors of difference in accuracy, or difference in reaction time. In a third model, we tested the degree to which PRI scores from the WASI were predictive of the five extracted peak differences. In all analyses we controlled for the effect of age during time 1 of the study. There was only one significant relationship that emerged, which indicated that differences in beta activity in the left superior temporal gyrus were related to PRI composite scores ($\beta = -.42$, b = −0.13, $p = .019$). Specifically, youth who had greater fluid intelligence as assessed by the WASI-II tended to exhibit stronger beta responses over time (i.e., greater decreases in power at time 2 relative to time 1). There were no significant relationships between any of the peaks and either changes in accuracy or changes in reaction time in the MEG task (note: full model results are available in supplemental Tables S1–S3). Thus, we further probed for relationships to changes in task behavior in a set of exploratory analyses.

3.4. Exploratory links to behavioral change

To identify links between oscillatory and behavioral changes between time 1 and time 2, we computed subtraction maps per person for the theta, beta, and gamma images, with the resultant maps indicating differences in oscillatory activity over time (time 2 minus time 1) across the entire brain. Using these subtraction maps, we computed whole-brain correlations between differences in neural oscillatory activity and changes in MEG task performance (i.e., accuracy and reaction time). In each correlation analysis, we covaried out the effect of age during time 1 of the study. We maintained the statistical and cluster thresholding from the main analyses. There were significant correlations between changes in theta activity and task accuracy within the right superior temporal ($r_{(30)} = .58$, $p = .001$) and precentral gyri ($r_{(30)} = .54$, $p = .003$), and within the left superior ($r_{(30)} = .56$, $p = .003$) and inferior frontal gyri ($r_{(30)} = .57$, $p = .002$; Fig. 6). The data indicated that above and beyond the effects of age, youth who had greater increases in theta activity over time in these regions also tended to have greater improvements in task accuracy. There was also a notable correlation between changes in accuracy and gamma activity. Namely, after accounting for age effects, youth who had decreased gamma activity within the right inferior temporal gyrus ($r_{(31)} = -.58$, $p = .001$) tended to show greater improvements in task accuracy over time.

With respect to changes in reaction time, there were significant associations with theta activity such that increases in theta within the left cuneus were associated with slower responses over time ($r_{(30)} = .57$, $p = .004$). Conversely, increases in theta within the right precentral ($r_{(30)} = -.55$, $p = .002$) and superior temporal gyri ($r_{(30)} = -.55$, $p = .002$), and increases in gamma in the left precentral gyrus ($r_{(31)} = -.58$, $p = .001$) and right inferior parietal cortex ($r_{(31)} = -.53$, $p = .004$) were all associated with faster reaction times (Fig. 7). Of note, theta peaks in the right precentral and superior temporal gyri closely overlapped with those observed for accuracy (Fig. 6).

4. Discussion

The present study examined longitudinal changes in neural oscillatory dynamics serving abstract reasoning among typically developing children and adolescents. Our key findings showed robust changes in the neural oscillatory dynamics across years of the study indicating reduced recruitment of compensatory, additional regions, and increased recruitment of areas commonly associated with efficient fluid reasoning in adults. We additionally saw that youths with greater fluid intelligence abilities measured by a traditional neuropsychological assessment tended to exhibit stronger beta oscillations (i.e., greater decreases in power relative to baseline) within the left superior temporal gyrus over time. Finally, we found multiple associations between changes in oscillatory power and changes in performance on the abstract reasoning task across years of the study. We discuss these findings in detail below.

Our data indicated a broad reduction in recruitment of the right lateral prefrontal cortex longitudinally. Specifically, the right prefrontal cortex showed robust theta oscillations at time 1 but was scarcely active in the subsequent year. In concert, youths exhibited significantly greater recruitment of the left inferior frontal and superior temporal cortices longitudinally, as indexed by the emergence of beta oscillations (i.e., decreases from

baseline or desynchronizations) at time 2. Importantly, although these changes in neural dynamics were not associated with performance during the MEG task, youths who showed greater recruitment of the left superior temporal gyrus over time tended to have greater fluid intelligence as indexed by a gold-standard neuropsychological assessment. Although we did not hypothesize shifts in beta oscillatory activity across years of the study, this finding is rather intuitive. Previous works have linked stronger beta responses (i.e., larger desynchronizations) to a number of higher order cognitive processes such as top-down attentional control (Koshy et al., 2020; Stoll et al., 2016). Further, recent works have distinctly implicated beta oscillations in processing finite local features of complex visual stimuli (Romei et al., 2011; Zaretskaya and Bartels, 2015). For instance, Zaretskaya and Bartels (2015) noted that local feature processing, relative to global stimulus processing, was characterized by stronger beta activity. It is possible that the shift in beta oscillatory responses noted in the present study reflected maturing local processing capabilities given the abstract reasoning task demands, which required youths to quickly dissect local features of complex visual stimuli.

On the other hand, we did detect additional changes in neural oscillatory dynamics that *were* specifically related to aspects of behavioral performance on the abstract reasoning task. Improvements in both accuracy and reaction times across years of the study were associated with shifts in theta and gamma activity across a distributed network, including key frontal and temporal regions frequently implicated in fluid reasoning (Jung and Haier, 2007). For example, increasing theta activity in the left inferior frontal gyrus was associated with greater accuracy on the task. As mentioned previously, the left inferior frontal gyrus is frequently highlighted for its role in fluid reasoning abilities in the mature adult brain (Basten et al., 2015; Jung and Haier, 2007). Coupled with the role of theta as a purveyor of long-range neural communication, including top-down attentional control mechanisms (Başar and Güntekin, 2013; Cavanagh and Frank, 2014; Colgin, 2013), it is sensible that we would see this pattern of maturation emerge in the present longitudinal study.

Interestingly, we saw close overlap in effects within the theta band, such that increasing theta power in the right precentral and superior temporal gyri was associated with improvements in both accuracy and reaction time across years of the study. These findings are supported by a broad body of literature examining links between theta oscillatory activity and motor performance. In a recent study, Muthukrishnan et al. (2020) explored changes in oscillatory dynamics in adults performing a working memory paradigm of varying load. They found that theta connectivity among distributed right hemisphere regions spanning parietal and temporal areas was diminished during high-load working memory conditions, and that reduction in theta connectivity was associated with poorer performance on the task (i.e., lower accuracy). Another study in individuals with Parkinson’s Disease showed that theta activity in the right superior temporal gyrus increased following transcranial magnetic stimulation therapy, and that this increase in theta activity was associated with improved motor outcomes (Tanaka et al., 2002). In general, the literature points to a key functional role of theta activity in these brain regions for optimizing both motor and cognitive performance.

With respect to gamma, we found that increasing gamma in the left precentral gyrus and right inferior parietal cortex was associated with faster reaction times across years of the study, areas that are commonly implicated in planning and executing motor responses (Chung et al., 2017; Spooner et al., 2021). It is possible that these effects reflect the upcoming motor response during the task, although the statistically-defined time bin for our gamma responses extended from 100 to 1000 ms after the stimulus onset, which was well before the group mean reaction time of ~1900 ms. Further, while the left precentral gyrus is the most common source of the motor-related gamma response to movements of the right hand/fingers, no studies to our knowledge have reported such responses in the parietal cortices (Heinrichs-Graham et al., 2018; Trevarrow et al., 2019; Wiesman et al., 2020). About the timing, there was a wide distribution of response times among the sample in both years of the study and some participants responded closer to the 1000 ms mark, which could help explain that discrepancy, at least for the left precentral gyrus response. Further investigation using motor response-locked analyses would shed more light on the nature of motor gamma in the current study, and its role in properly processing and performing the abstract reasoning task.

Taken together, these data support previous literature suggesting a fundamental reconfiguration of functional networks underlying fluid reasoning across child and adolescent development (Fuhrmann et al., 2019; Menon, 2013; Simpson-Kent et al., 2020). More specifically, our developmental data illustrate reduced recruitment of brain regions that are not as strongly linked to fluid reasoning (e.g., *right* lateral prefrontal cortex), along with increased recruitment of areas known to be critical for fluid reasoning among mature adults (e.g., left inferior frontal gyrus; Basten et al., 2015; Jung and Haier, 2007). The overall network of regions showing oscillatory change over time in the present study closely resembles that of a recent fMRI/PET-based meta-analysis reporting the neural regions critical for fluid reasoning among primarily older adolescents and young adults (Santarnecchi et al., 2017). Other studies have also reported developmental changes in functional brain activity, with or without changes in behavioral performance, across multiple cognitive domains including relational reasoning (Dumontheil et al., 2010), executive functioning (Guevara et al., 2013), and attentional processing (Taylor et al., 2019, 2016). Such findings are believed to reflect shifts in neurocognitive strategies as learning and development occur. Indeed, a seminal study by Uhlhaas et al. (2009) showed that shifts in synchronization specifically within theta, beta, and gamma bands from childhood into adulthood are indicative of restructured functional networks during development. Such a shift is consistent with the functional roles of these different oscillatory bands in the mature brain. Theta and beta oscillatory responses have been repeatedly implicated in the coordination of long-range neural communication (e.g., between frontal and parietal areas) during higher order cognitive processing (Engel and Fries, 2010; Schnitzler and Gross, 2005; Spitzer and Haegens, 2017; Uhlhaas et al., 2008), whereas gamma activity is believed to be critical for local information maintenance and integration during complex tasks (Gregoriou et al., 2009; Mellem et al., 2013; Uhlhaas et al., 2008). Thus, framing the data acquired in the current study in the context of the extant literature, our data may be suggestive of improved performance through the reconfiguration of functional networks serving fluid reasoning, as indicated by changes in long-range communication across key

regions involved in fluid reasoning, and critical local maintenance and processing of the complex stimuli in the abstract reasoning task.

Before closing, we must address several limitations of the current study. First, we had a relatively limited number of youths who successfully completed the abstract reasoning task at both time points. Further, the sample was not perfectly balanced, with a greater proportion of male participants in the final sample. Given the smaller, somewhat imbalanced sample size, we were limited in the breadth and depth of analyses we were able to perform, including explorations of sex-specific changes in neural oscillatory dynamics over time. Several recent studies have shown unique trajectories of development among male versus female youths in investigations of both task-based (Fung et al., 2021; Taylor et al., 2021, 2020) and spontaneous cortical dynamics (Ott et al., 2021). Future longitudinal studies should aim to acquire data from larger samples of equally-balanced male and female youths to further disentangle the unique trajectories of fluid reasoning maturation in this dynamic period of development. It would also be fruitful to explore additional time points to better model non-linear patterns of longitudinal development. It goes without saying that longitudinal data sets are rich in nature, and the analytic approach utilized in the current investigation was one of many possible avenues for understanding the nature of maturation in neural oscillatory dynamics. Future investigations should incorporate additional statistical tools to further probe changes in neural processing during adolescence. For instance, linear mixed effects modeling would allow for more individualized approaches to understanding changes in neural oscillations over time as a function of age at the start of the study. Further, dynamic functional connectivity analyses may reveal shifts in brain network organization that were not obvious in the current statistical design. Future studies could also employ more regional approaches to identifying whether specific oscillatory responses exhibit clear relationships to behavioral performance and/or general cognitive abilities. While we tested both peak voxel and local cluster methods and found the conclusions to be identical, inflating the region even more broadly may illuminate new relationships. Finally, we only explored changes in neural dynamics during an abstract reasoning task. Although this is a common type of assessment for fluid reasoning, there are many ways to assess fluid intelligence abilities that entail varying cognitive demands and stimulus types. Thus, while our data provide a unique view into the within-person developmental changes in oscillatory dynamics serving abstract reasoning, these findings may not be fully generalizable to the broader construct of fluid intelligence.

To conclude, the present study is one of a limited number to quantify longitudinal changes in abstract reasoning abilities in children and adolescents. We found distributed shifts in theta, beta, and gamma oscillatory activity during the task, which largely indicated decreased recruitment of areas that are rarely linked to fluid reasoning in adults (e.g., right lateral prefrontal cortex), and increased recruitment of regions classically implicated in fluid reasoning among such mature adults (e.g., left frontal and parietal regions). Importantly, such changes in oscillatory dynamics were associated with fluid intelligence measured by a gold-standard neuropsychological assessment, and with improvements in accuracy and reaction time across years of the study. These data may reflect critical developmental changes in the reconfiguration and timing of the functional brain dynamics underlying fluid intelligence among children and adolescents.

Supplementary Material

Refer to Web version on PubMed Central for supplementary material.

Acknowledgments

This work was supported by the National Science Foundation of the USA (#1539067 and 2112455) and the National Institutes of Health (R01-MH121101, R01-MH116782, P20-GM144641). The funders had no role in study design, data collection and analysis, decision to publish, or preparation of the manuscript.

Data availability

The data used in this article are openly available through the COINS framework (https://coins.trendscenter.org/). See dataset COINS:Dev-CoG. Those who wish to use the data can create an account with COINS and complete a data request process for the study, similar to other major open access data repositories.

References

Başar E, Güntekin B, 2013. Review of delta, theta, alpha, beta, and gamma response oscillations in neuropsychiatric disorders. Suppl. Clin. Neurophysiol. 303–341. doi: 10.1016/B978-0-7020-5307-8.00019-3, Elsevier. [PubMed: 24053047]

Basten U, Hilger K, Fiebach CJ, 2015. Where smart brains are different: a quantitative meta-analysis of functional and structural brain imaging studies on intelligence. Intelligence 51, 10–27. doi: 10.1016/j.intell.2015.04.009.

Bazargani N, Hillebrandt H, Christoff K, Dumontheil I, 2014. Developmental changes in effective connectivity associated with relational reasoning. Hum. Brain Mapp. 35, 3262–3276. doi: 10.1002/hbm.22400. [PubMed: 25050424]

Casey BJ, Giedd JN, Thomas KM, 2000. Structural and functional brain development and its relation to cognitive development. Biol. Psychol. 54, 241–257. doi: 10.1016/S0301-0511(00)00058-2. [PubMed: 11035225]

Cavanagh JF, Figueroa CM, Cohen MX, Frank MJ, 2012. Frontal theta reflects uncertainty and unexpectedness during exploration and exploitation. Cereb. Cortex 22, 2575–2586. doi: 10.1093/cercor/bhr332. [PubMed: 22120491]

Cavanagh JF, Frank MJ, 2014. Frontal theta as a mechanism for cognitive control. Trends Cogn. Sci. 18, 414–421. doi: 10.1016/j.tics.2014.04.012. [PubMed: 24835663]

Chung JW, Ofori E, Misra G, Hess CW, Vaillancourt DE, 2017. Beta-band activity and connectivity in sensorimotor and parietal cortex are important for accurate motor performance. Neuroimage 144, 164–173. doi: 10.1016/j.neuroimage.2016.10.008. [PubMed: 27746389]

Cohen MX, Ridderinkhof KR, 2013. EEG source reconstruction reveals frontal-parietal dynamics of spatial conflict processing. PLoS One 8, e57293. doi: 10.1371/journal.pone.0057293. [PubMed: 23451201]

Colgin LL, 2013. Mechanisms and functions of theta rhythms. Annu. Rev. Neurosci. 36, 295–312. doi: 10.1146/annurev-neuro-062012-170330. [PubMed: 23724998]

Conway ARA, Cowan N, Bunting MF, Therriault DJ, Minkoff SRB, 2002. A latent variable analysis of working memory capacity, short-term memory capacity, processing speed, and general fluid intelligence. Intelligence 30, 163–183. doi: 10.1016/S0160-2896(01)00096-4.

Crone EA, Ridderinkhof RK, 2011. The developing brain: From theory to neuroimaging and back. Dev. Cogn. Neurosci. 1, 101–109. doi: 10.1016/j.dcn.2010.12.001. [PubMed: 22436435]

Dix A, Wartenburger I, van der Meer E, 2016. The role of fluid intelligence and learning in analogical reasoning: how to become neurally efficient? Neurobiol. Learn. Mem. 134, 236–247. doi: 10.1016/j.nlm.2016.07.019. [PubMed: 27461735]

Dumontheil I, 2014. Development of abstract thinking during childhood and adolescence: the role of rostrolateral prefrontal cortex. Dev. Cogn. Neurosci. 10, 57–76. doi: 10.1016/j.dcn.2014.07.009. [PubMed: 25173960]

Dumontheil I, Houlton R, Christoff K, Blakemore SJ, 2010. Development of relational reasoning during adolescence: relational reasoning development. Dev. Sci. 13, F15–F24. doi: 10.1111/j.1467-7687.2010.01014.x. [PubMed: 20977551]

Engel AK, Fries P, 2010. Beta-band oscillations—signalling the status quo? Curr. Opin. Neurobiol. 20, 156–165. doi: 10.1016/j.conb.2010.02.015. [PubMed: 20359884]

Ernst MD, 2004. Permutation methods: a basis for exact inference. Stat. Sci. 19, 676–685. doi: 10.1214/088342304000000396.

Estrada E, Ferrer E, Román FJ, Karama S, Colom R, 2019. Time-lagged associations between cognitive and cortical development from childhood to early adulthood. Dev. Psychol. doi: 10.1037/dev0000716.

Feldstein Ewing SW, Bjork JM, Luciana M, 2018. Implications of the ABCD study for developmental neuroscience. Dev. Cogn. Neurosci. 32, 161–164. doi: 10.1016/j.dcn.2018.05.003, The Adolescent Brain Cognitive Development (ABCD) Consortium: Rationale, Aims, and Assessment Strategy. [PubMed: 29773510]

Ferrer E, O'Hare ED, Bunge SA, 2009. Fluid reasoning and the developing brain. Front. Neurosci. 3. doi: 10.3389/neuro.01.003.2009.

Fuhrmann D, Simpson-Kent IL, Bathelt J, Team, The CALM, Holmes J, Gather-cole S, Astle D, Manly T, Kievit R, Kievit RA, 2019. A hierarchical water-shed model of fluid intelligence in childhood and adolescence. Cereb. Cortex bhz091 doi: 10.1093/cercor/bhz091.

Fung MH, Taylor BK, Lew BJ, Frenzel MR, Eastman JA, Wang Y-P, Calhoun VD, Stephen JM, Wilson TW, 2021. Sexually dimorphic development in the cortical oscillatory dynamics serving early visual processing. Dev. Cogn. Neurosci. 50, 100968. doi: 10.1016/j.dcn.2021.100968. [PubMed: 34102602]

Gottfredson LS, Deary IJ, 2004. Intelligence predicts health and longevity, but why? Curr. Dir. Psychol. Sci. 13, 1–4. doi: 10.1111/j.0963-7214.2004.01301001.x.

Gregoriou GG, Gotts SJ, Zhou H, Desimone R, 2009. High-frequency, long-range coupling between prefrontal and visual cortex during attention. Science 324, 1207–1210. doi: 10.1126/science.1171402. [PubMed: 19478185]

Gross J, Kujala J, Hämäläinen M, Timmermann L, Schnitzler A, Salmelin R, 2001. Dynamic imaging of coherent sources: studying neural interactions in the human brain. Proc. Natl. Acad. Sci. 98, 694–699. doi: 10.1073/pnas.98.2.694. [PubMed: 11209067]

Guevara MÁ, Hernández González M, Rizo Martínez LE, Robles Aguirre FA, 2013. Performance of the towers of Hanoi task and cortical electroencephalographic power changes associated with infancy, adolescence, and early adulthood. Exp. Brain Res. 231, 315–324. doi: 10.1007/s00221-013-3693-z. [PubMed: 24013790]

Heinrichs-Graham E, Hoburg JM, Wilson TW, 2018. The peak frequency of motor-related gamma oscillations is modulated by response competition. Neuroimage 165, 27–34. doi: 10.1016/j.neuroimage.2017.09.059. [PubMed: 28966082]

Hillebrand A, Singh KD, Holliday IE, Furlong PL, Barnes GR, 2005. A new approach to neuroimaging with magnetoencephalography. Hum. Brain Mapp. 25, 199–211. doi: 10.1002/hbm.20102. [PubMed: 15846771]

Hobeika L, Diard-Detoeuf C, Garcin B, Levy R, Volle E, 2016. General and specialized brain correlates for analogical reasoning: a meta-analysis of functional imaging studies. Hum. Brain Mapp. 37, 1953–1969. doi: 10.1002/hbm.23149. [PubMed: 27012301]

Jensen O, Tesche CD, 2002. Frontal theta activity in humans increases with memory load in a working memory task. Eur. J. Neurosci. 15, 1395–1399. doi: 10.1046/j.1460-9568.2002.01975.x. [PubMed: 11994134]

Jernigan TL, Brown SA, Dowling GJ, 2018. The adolescent brain cognitive development study. J. Res. Adolesc. Off. J. Soc. Res. Adolesc. 28, 154–156. doi: 10.1111/jora.12374.

Jung RE, Haier RJ, 2007. The parieto-frontal integration theory (p-fit) of intelligence: converging neuroimaging evidence. Behav Brain Sci 30, 135–154. doi: 10.1017/S0140525X07001185. [PubMed: 17655784]

Kievit RA, Fuhrmann D, Borgeest GS, Simpson-Kent IL, Henson RNA, 2018. The neural determinants of age-related changes in fluid intelligence: a pre-registered, longitudinal analysis in UK Biobank. Wellcome Open Res. 3. doi: 10.12688/wellcomeopenres.14241.2.

Kievit RA, Simpson-Kent IL, 2021. It's about Time: Towards a Longitudinal Cognitive Neuroscience of Intelligence. In: Barbey AK, Haier RJ, Karama S (Eds.), The Cambridge Handbook of Intelligence and Cognitive Neuroscience. Cambridge University Press, Cambridge, pp. 123–146. doi: 10.1017/9781108635462.010.

Koshy SM, Wiesman AI, Proskovec AL, Embury CM, Schantell MD, Eastman JA, Heinrichs-Graham E, Wilson TW, 2020. Numerical working memory alters alpha-beta oscillations and connectivity in the parietal cortices. Hum. Brain Mapp. 41, 3709–3719. doi: 10.1002/hbm.25043. [PubMed: 32459874]

Maris E, Oostenveld R, 2007. Nonparametric statistical testing of EEG- and MEG-data. J. Neurosci. Methods 164, 177–190. doi: 10.1016/j.jneumeth.2007.03.024. [PubMed: 17517438]

Mcardle JJ, Ferrer-caja E, Hamagami F, Woodcock RW, Cattell RB, Data T, 2002. Comparative longitudinal structural analyses of the growth and decline of multiple intellectual abilities over the life span. Dev. Psychol..

McDermott TJ, Badura-Brack AS, Becker KM, Ryan TJ, Bar-Haim Y, Pine DS, Khanna MM, Heinrichs-Graham E, Wilson TW, 2016a. Attention training improves aberrant neural dynamics during working memory processing in veterans with PTSD. Cogn. Affect. Behav. Neurosci. 16, 1140–1149. doi: 10.3758/s13415-016-0459-7. [PubMed: 27722837]

McDermott TJ, Badura-Brack AS, Becker KM, Ryan TJ, Khanna MM, Heinrichs-Graham E, Wilson TW, 2016b. Male veterans with PTSD exhibit aberrant neural dynamics during working memory processing: An MEG study. J. Psychiatry Neurosci. 41, 251–260. doi: 10.1503/jpn.150058 [PubMed: 26645740]

Mellem MS, Friedman RB, Medvedev AV, 2013. Gamma- and theta-band synchronization during semantic priming reflect local and long-range lexical-semantic networks. Brain Lang. 127. doi: 10.1016/j.bandl.2013.09.003.

Menon V, 2013. Developmental pathways to functional brain networks: emerging principles. Trends Cogn. Sci. 17, 627–640. doi: 10.1016/j.tics.2013.09.015. [PubMed: 24183779]

Meyer L, Obleser J, Friederici AD, 2013. Left parietal alpha enhancement during working memory-intensive sentence processing. Cortex 49, 711–721. doi: 10.1016/j.cortex.2012.03.006. [PubMed: 22513340]

Muthukrishnan SP, Soni S, Sharma R, 2020. Brain networks communicate through theta oscillations to encode high load in a visuospatial working memory task: an EEG connectivity study. Brain Topogr. 33, 75–85. doi: 10.1007/s10548-019-00739-3. [PubMed: 31650366]

Neubauer AC, Fink A, 2003. Fluid intelligence and neural efficiency: effects of task complexity and sex. Pers. Individ. Differ. 35, 811–827. doi: 10.1016/S0191-8869(02)00285-4.

Neubauer AC, Wammerl M, Benedek M, Jauk E, Jaušovec N, 2017. The influence of transcranial alternating current stimulation (tACS) on fluid intelligence: an fMRI study. Personal. Individ. Differ. 118, 50–55. doi: 10.1016/j.paid.2017.04.016, Robert Stelmack: Differential Psychophysiology.

Ott LR, Penhale SH, Taylor BK, Lew BJ, Wang YP, Calhoun VD, Stephen JM, Wilson TW, 2021. Spontaneous cortical MEG activity undergoes unique age- and sex-related changes during the transition to adolescence. Neuroimage 244, 118552. doi: 10.1016/j.neuroimage.2021.118552. [PubMed: 34517128]

Pahor A, Jaušovec N, 2014. The effects of theta transcranial alternating current stimulation (tACS) on fluid intelligence. Int. J. Psychophysiol. 93, 322–331. doi: 10.1016/j.ijpsycho.2014.06.015. [PubMed: 24998643]

Perfetti B, Saggino A, Ferretti A, Caulo M, Romani GL, 2009. Differential patterns of cortical activation as a function of fluid reasoning complexity. Hum. Brain Mapp. Onofrj, M, 30, 497–510. doi: 10.1002/hbm.20519.

Phillips S, Takeda Y, 2009. Greater frontal-parietal synchrony at low gamma-band frequencies for inefficient than efficient visual search in human EEG. Int. J. Psychophysiol. 73, 350–354. doi: 10.1016/j.ijpsycho.2009.05.011. [PubMed: 19481120]

Rajan A, Siegel SN, Liu Y, Bengson J, Mangun GR, Ding M, 2018. Theta oscillations index frontal decision-making and mediate reciprocal frontal–parietal interactions in willed attention. Cereb. Cortex doi: 10.1093/cercor/bhy149.

Ramchandran K, Zeien E, Andreasen NC, 2019. Distributed neural efficiency: intelligence and age modulate adaptive allocation of resources in the brain. Trends Neurosci. Educ. doi: 10.1016/j.tine.2019.02.006.

Ramos J, Corsi-Cabrera M, Guevara MA, Arce C, 1993. EEG activity during cognitive performance in women. Int. J. Neurosci. 69, 185–195. doi: 10.3109/00207459309003329. [PubMed: 8083005]

Romei V, Driver J, Schyns PG, Thut G, 2011. Rhythmic TMS over parietal cortex links distinct brain frequencies to global versus local visual processing. Curr. Biol. 21, 334–337. doi: 10.1016/j.cub.2011.01.035. [PubMed: 21315592]

Rosen A, Reiner M, 2017. Right frontal gamma and beta band enhancement while solving a spatial puzzle with insight. Int. J. Psychophysiol. 122, 50–55. doi: 10.1016/j.ijpsycho.2016.09.008. [PubMed: 27671505]

Sadaghiani S, Scheeringa R, Lehongre K, Morillon B, Giraud A-L, D'Esposito M, Kleinschmidt A, 2012. Alpha-band phase synchrony is related to activity in the fronto-parietal adaptive control network. J. Neurosci. 32, 14305–14310. doi: 10.1523/JNEUROSCI.1358-12.2012. [PubMed: 23055501]

Santarnecchi E, Emmendorfer A, Pascual-Leone A, 2017. Dissecting the parieto-frontal correlates of fluid intelligence: a comprehensive ALE meta-analysis study. Intelligence 63, 9–28. doi: 10.1016/j.intell.2017.04.008.

Santarnecchi E, Muller T, Rossi S, Sarkar A, Polizzotto NR, Rossi A, Cohen Kadosh R, 2016. Individual differences and specificity of prefrontal gamma frequency-tACS on fluid intelligence capabilities. Cortex 75, 33–43. doi: 10.1016/j.cortex.2015.11.003. [PubMed: 26707084]

Santarnecchi E, Polizzotto NR, Godone M, Giovannelli F, Feurra M, Matzen L, Rossi A, Rossi S, 2013. Frequency-dependent enhancement of fluid intelligence induced by transcranial oscillatory potentials. Curr. Biol. 23, 1449–1453. doi: 10.1016/j.cub.2013.06.022. [PubMed: 23891115]

Sauseng P, Klimesch W, Schabus M, Doppelmayr M, 2005. Fronto-parietal EEG coherence in theta and upper alpha reflect central executive functions of working memory. Int. J. Psychophysiol. 57, 97–103. doi: 10.1016/j.ijpsycho.2005.03.018. [PubMed: 15967528]

Schnitzler A, Gross J, 2005. Normal and pathological oscillatory communication in the brain. Nat. Rev. Neurosci. 6, 285–296. doi: 10.1038/nrn1650. [PubMed: 15803160]

Shaw P, 2007. Intelligence and the developing human brain. Bioessays 29, 962–973. doi: 10.1002/bies.20641. [PubMed: 17876781]

Simpson-Kent IL, Fuhrmann D, Bathelt J, Achterberg J, Borgeest GS, Kievit RA, 2020. Neurocognitive reorganization between crystallized intelligence, fluid intelligence and white matter microstructure in two age-heterogeneous developmental cohorts. Dev. Cogn. Neurosci. 41, 100743. doi: 10.1016/j.dcn.2019.100743. [PubMed: 31999564]

Spitzer B, Haegens S, 2017. Beyond the status quo: a role for beta oscillations in endogenous content (Re) activation. eNeuro 4, 1–15. doi: 10.1523/ENEURO.0170-17.2017.

Spooner RK, Arif Y, Taylor BK, Wilson TW, 2021. Movement-related gamma synchrony differentially predicts behavior in the presence of visual interference across the lifespan. Cereb. Cortex 31, 5056–5066. doi: 10.1093/cercor/bhab141, N. Y. N 1991. [PubMed: 34115110]

Stephen JM, Solis I, Janowich J, Stern M, Frenzel MR, Eastman JA, Mills MS, Embury CM, Coolidge NM, Heinrichs-Graham E, Mayer A, Liu J, Wang YP, Wilson TW, Calhoun VD, 2021. The developmental chronnecto-genomics (Dev-CoG) study: a multimodal study on the developing brain. Neuroimage 225, 117438. doi: 10.1016/j.neuroimage.2020.117438. [PubMed: 33039623]

Stoll FM, Wilson CRE, Faraut MCM, Vezoli J, Knoblauch K, Procyk E, 2016. The effects of cognitive control and time on frontal beta oscillations. Cereb. Cortex 26, 1715–1732. doi: 10.1093/cercor/bhv006. [PubMed: 25638168]

Tanaka H, Ebata A, Arai M, Ito M, Harada M, Yamazaki K, Hirata K, 2002. Evaluation of transcranial magnetic stimulation for depressed Parkinson's disease with LORETA. Int. Congr. Ser. 901–905. doi: 10.1016/S0531-5131(01)00843-3, Recent advances in human brain mapping 1232.

Taulu S, Simola J, 2006. Spatiotemporal signal space separation method for rejecting nearby interference in MEG measurements. Phys. Med. Biol. 51, 1759–1768. doi: 10.1088/0031-9155/51/7/008. [PubMed: 16552102]

Taulu S, Simola J, Kajola M, 2005. Applications of the signal space separation method. IEEE Trans. Signal Process 53, 3359–3372. doi: 10.1109/TSP.2005.853302.

Taylor BK, Eastman JA, Frenzel MR, Embury CM, Wang Y-P, Calhoun VD, Stephen JM, Wilson TW, 2021. Neural oscillations underlying selective attention follow sexually divergent developmental trajectories during adolescence. Dev. Cogn. Neurosci. 49, 100961. doi: 10.1016/j.dcn.2021.100961. [PubMed: 33984667]

Taylor BK, Embury CM, Heinrichs-Graham E, Frenzel MR, Eastman JA, Wiesman AI, Wang YP, Calhoun VD, Stephen JM, Wilson TW, 2020. Neural oscillatory dynamics serving abstract reasoning reveal robust sex differences in typically-developing children and adolescents. Dev. Cogn. Neurosci 100770. doi: 10.1016/j.dcn.2020.100770. [PubMed: 32452465]

Taylor BK, Gavin WJ, Davies PL, 2016. The Test–retest reliability of the visually evoked contingent negative variation (CNV) in children and adults. Dev. Neuropsychol. 41, 162–175. [PubMed: 27145115]

Taylor BK, Gavin WJ, Grimm KJ, Prince MA, Lin MH, Davies PL, 2019. Towards a unified model of event-related potentials as phases of stimulus-to-response processing. Neuropsychologia 132, 107128. doi: 10.1016/j.neuropsychologia.2019.107128. [PubMed: 31229538]

Trevarrow MP, Kurz MJ, McDermott TJ, Wiesman AI, Mills MS, Wang Y-P, Calhoun VD, Stephen JM, Wilson TW, 2019. The developmental trajectory of sensorimotor cortical oscillations. Neuroimage 184, 455–461. doi: 10.1016/j.neuroimage.2018.09.018. [PubMed: 30217545]

Uhlhaas PJ, Haenschel C, Nikolić D, Singer W, 2008. The role of oscillations and synchrony in cortical networks and their putative relevance for the pathophysiology of schizophrenia. Schizophr. Bull. 34, 927–943. doi: 10.1093/schbul/sbn062. [PubMed: 18562344]

Uhlhaas PJ, Roux F, Singer W, Haenschel C, Sireteanu R, Rodriguez E, 2009. The development of neural synchrony reflects late maturation and restructuring of functional networks in humans. Proc. Natl. Acad. Sci. 106, 9866–9871. doi: 10.1073/pnas.0900390106. [PubMed: 19478071]

Uusitalo MA, Ilmoniemi RJ, 1997. Signal-space projection method for separating MEG or EEG into components. Med. Biol. Eng. Comput. 35, 135–140. doi: 10.1007/BF02534144. [PubMed: 9136207]

Veen BDV, Drongelen WV, Yuchtman M, Suzuki A, 1997. Localization of brain electrical activity via linearly constrained minimum variance spatial filtering. IEEE Trans. Biomed. Eng. 44, 867–880. doi: 10.1109/10.623056. [PubMed: 9282479]

Wascher E, Rasch B, Sänger J, Hoffmann S, Schneider D, Rinkenauer G, Heuer H, Gutberlet I, 2014. Frontal theta activity reflects distinct aspects of mental fatigue. Biol. Psychol. 96, 57–65. doi: 10.1016/j.biopsycho.2013.11.010. [PubMed: 24309160]

Wechsler D, 2011. WASI-II: Wechsler Abbreviated Scale of Intelligence. PsychCorp.

Wendelken C, Ferrer E, Ghetti S, Bailey S, Cutting L, Bunge SA, 2017. Fronto-parietal structural connectivity in childhood predicts development of functional connectivity and reasoning ability: a large-scale longitudinal investigation. J. Neurosci. 3716–3726. doi: 10.1523/JNEUROSCI.3726-16.2017.

Wendelken C, Ferrer E, Whitaker KJ, Bunge SA, 2016. Fronto-parietal network reconfiguration supports the development of reasoning ability. Cereb. Cortex 26, 2178–2190. doi: 10.1093/cercor/bhv050. [PubMed: 25824536]

Wierenga LM, Langen M, Oranje B, Durston S, 2014. Unique developmental trajectories of cortical thickness and surface area. Neuroimage 87, 120–126. doi: 10.1016/j.neuroimage.2013.11.010. [PubMed: 24246495]

Wiesman AI, Koshy SM, Heinrichs-Graham E, Wilson TW, 2020. Beta and gamma oscillations index cognitive interference effects across a distributed motor network. Neuroimage 213, 116747. doi: 10.1016/j.neuroimage.2020.116747. [PubMed: 32179103]

Wilson TW, Heinrichs-Graham E, Proskovec AL, McDermott TJ, 2016. Neuroimaging with magnetoencephalography: a dynamic view of brain pathophysiology. Transl. Res. J. Lab. Clin. Med. 175, 17–36. doi: 10.1016/j.trsl.2016.01.007.

Zaretskaya N, Bartels A, 2015. Gestalt perception is associated with reduced parietal beta oscillations. Neuroimage 112, 61–69. doi: 10.1016/j.neuroimage.2015.02.049. [PubMed: 25731988]

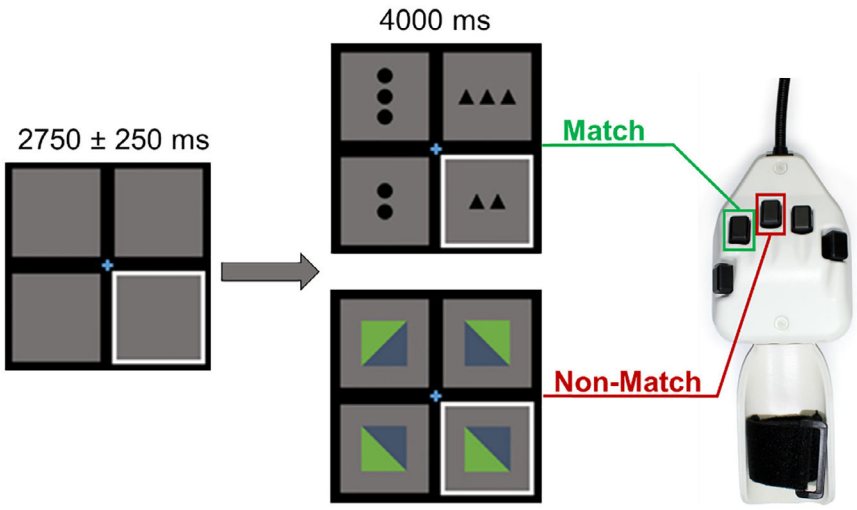

Fig. 1.

The abstract reasoning task. Participants were presented with an empty grid of gray boxes for 2500 to 3000 ms, during which time either the left or right bottom square was highlighted in white indicating the location of the upcoming target. Then, the grid populated with complex figures for 4000 ms. Participants indicated with a corresponding button press whether the image in the highlighted box correctly completed the pattern in the grid (i.e., “match”; 60 trials), or incorrectly completed the pattern in the grid (i.e., “non-match”; 60 trials). Match and non-match trials were pseudo-randomly presented for the duration of the task, with a 30 s break halfway through the paradigm.

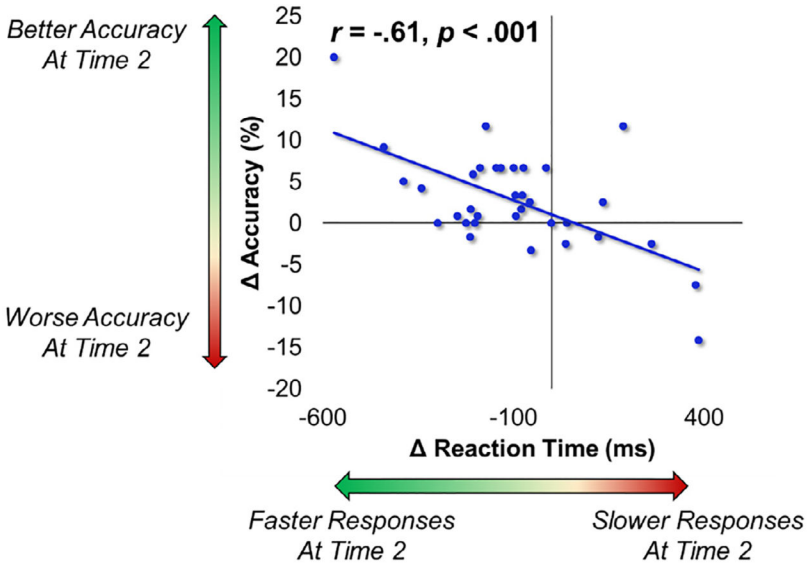

Fig. 2.

Association between changes in reaction time and changes in accuracy. Arrows alongside the x- and y-axes indicate the interpretation of effects. The differences in task accuracy and average reaction time over years of the study (Time 2 – Time 1) were negatively correlated, suggesting that youths who improved in accuracy over time also tended to respond faster over time.

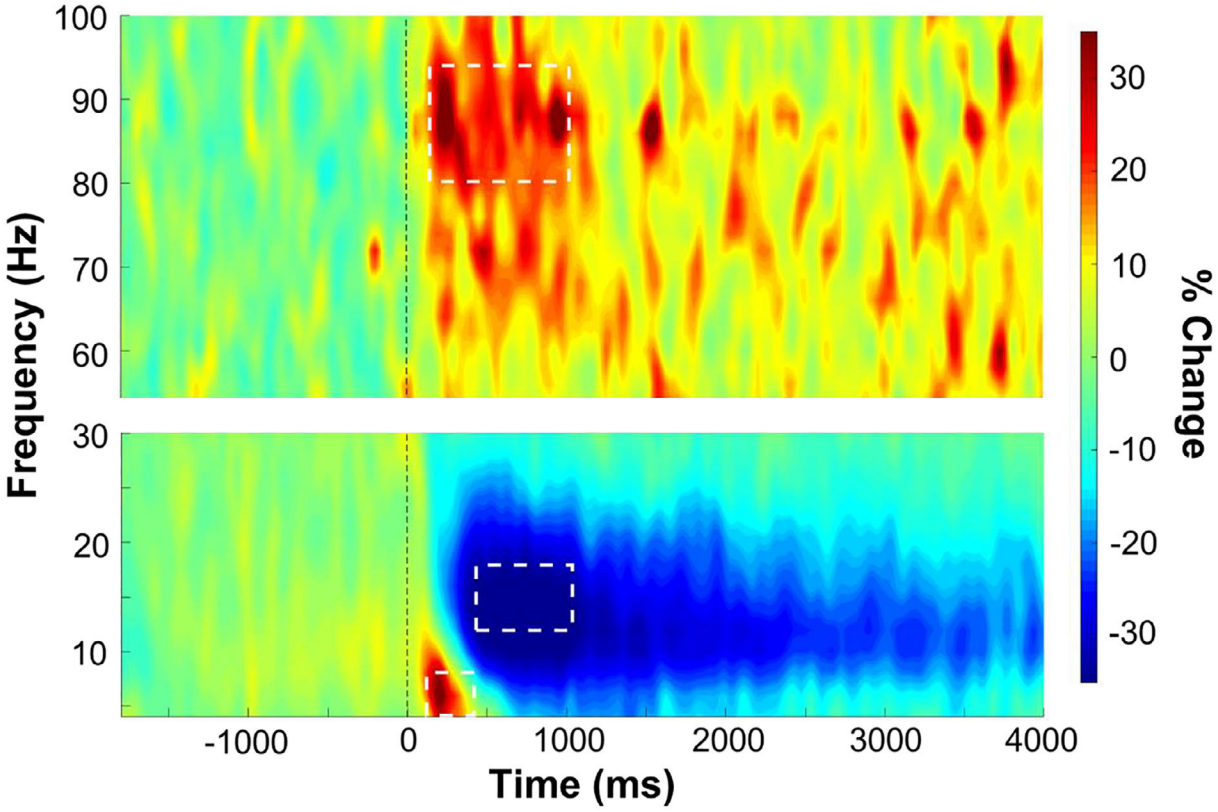

Fig. 3.

Spectrograms of significant periods of oscillatory activity during the abstract reasoning task, collapsed across years of the study. Using time frequency decomposition and permutation-corrected statistical analysis ($p < .05$, corrected), we detected three time-frequency bins with significant responses relative to baseline during the period of interest (i.e., the first 1000 ms following stimulus presentation). These included theta activity (4–8 Hz) from 100 to 400 ms, beta activity (12–18 Hz) from 400 to 1000 ms, and gamma activity (80–94 Hz) from 100 to 1000 ms. Here we show the gradiometers most clearly showing the response (i.e., M2232 for theta and beta, and M2032 for gamma), though all gradiometers were included in the statistical analyses.

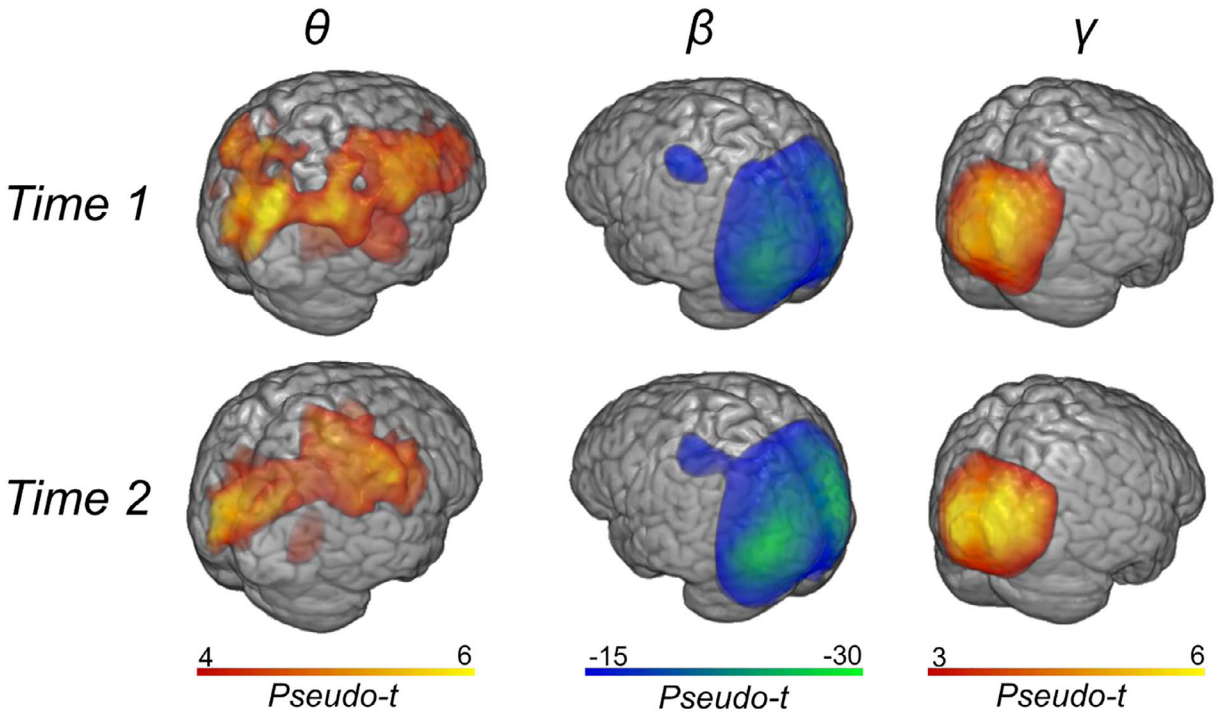

Fig. 4.

Averaged maps of oscillatory activity in each year of the study. Increased theta oscillations were broadly distributed across frontal, parietal, and occipital portions of the cortex and notably diminished at time 2. Beta oscillations appeared predominantly in occipital and parietal cortices, with a peak in the left parietal lobule. Activity appeared stronger at time 2. Finally, gamma responses were more focal and restricted to occipital cortices, with comparable activity at both time points.

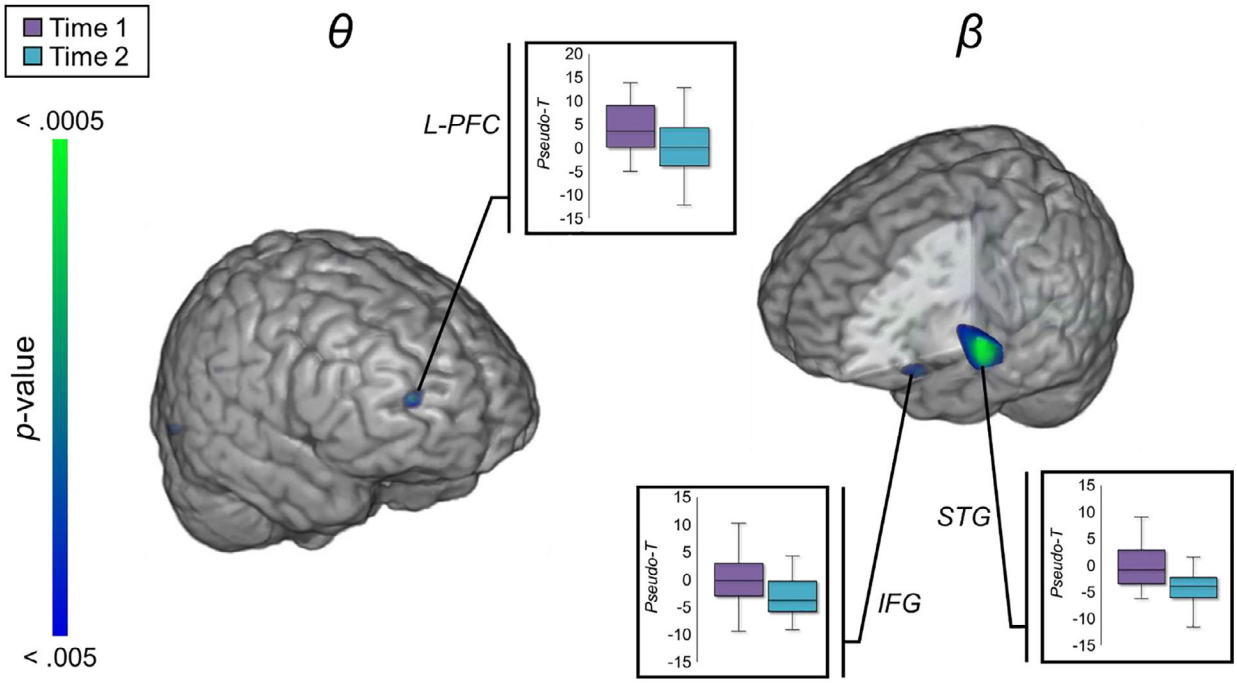

Fig. 5.

Differences in oscillatory activity across years of the study. Paired-samples t-tests comparing oscillatory activity at time 2 to time 1 revealed differences in theta and beta activity. Youths exhibited significantly reduced theta in right lateral prefrontal (left) and occipital areas (not shown), and significantly stronger beta responses in the left superior temporal and inferior frontal gyri (right), as well as the right parahippocampal gyrus (not shown). L-PFC: lateral prefrontal cortex; IFG: inferior frontal gyrus; STG: superior temporal gyrus.

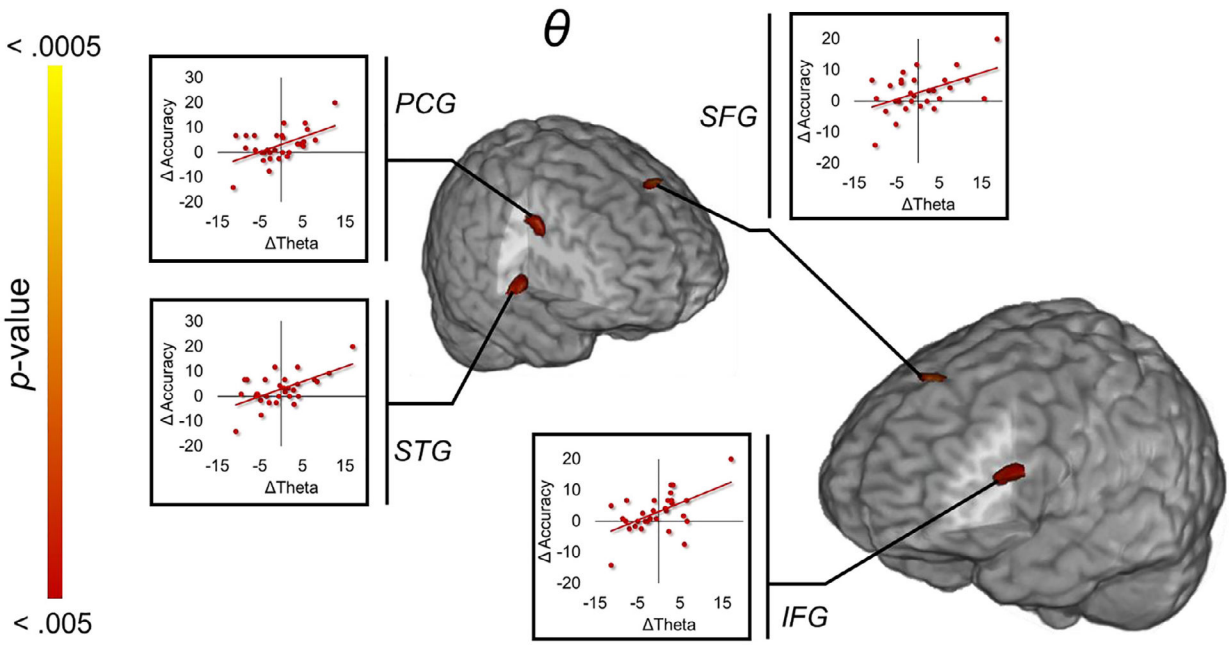

Fig. 6.

Neural dynamics associated with changes in task accuracy. We correlated the difference in overall task accuracy (time 2 – time 1) with theta, beta, and gamma oscillatory subtraction maps (time 2 – time 1), controlling for the effect of age in each analysis. There were no significant associations between changes in accuracy and changes in beta activity over time that survived our conservative thresholding. However, we saw several correlations between changes in accuracy and shifts in both theta and gamma oscillatory activity. Overall, increases in theta activity and decreases in gamma activity (not shown) were associated with improvements in task accuracy. PCG: precentral gyrus; STG: superior temporal gyrus: IFG: inferior frontal gyrus; SFG: superior frontal gyrus.

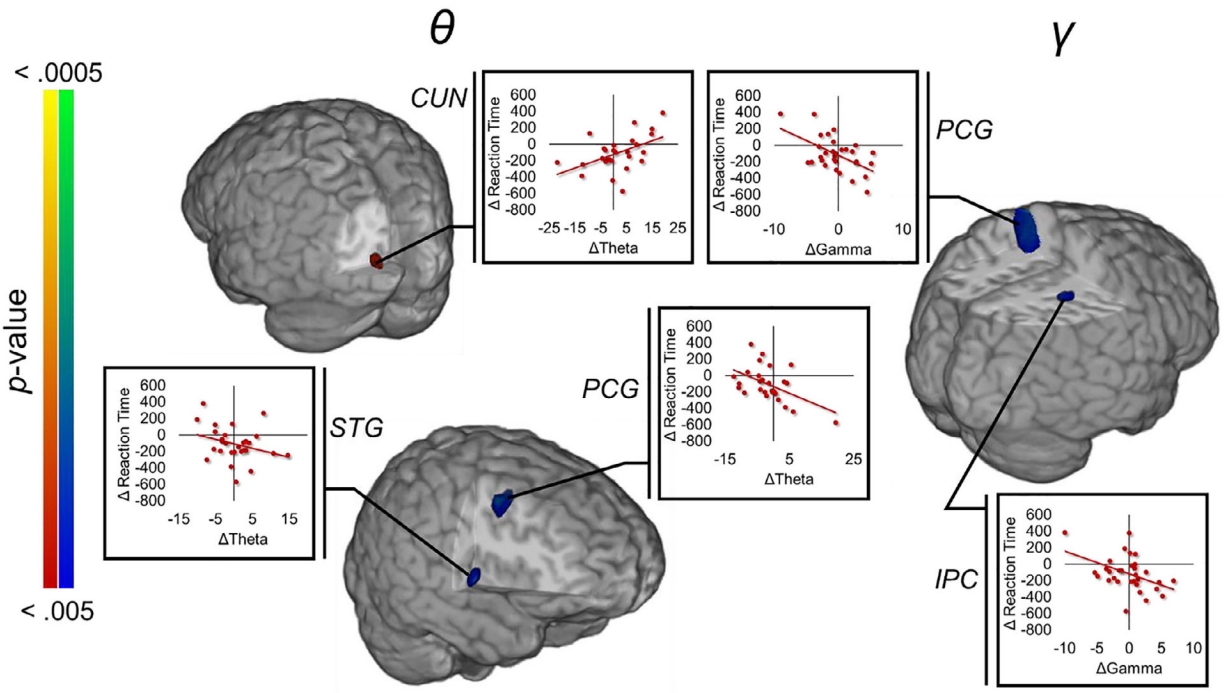

Fig. 7.

Neural dynamics associated with changes in reaction times. We correlated the difference in averaged reaction times (time 2 – time 1) with theta, beta, and gamma oscillatory subtraction maps, controlling for the effect of age in each analysis. As was seen for accuracy, there were no significant associations between changes in reaction time and changes in beta activity over time. However, several correlations were detected between changes in reaction times and shifts in theta and gamma oscillatory activity. Increases in both theta and gamma response strengths over time were associated with faster response times in the right inferior parietal cortices, right superior temporal gyrus, and bilateral precentral gyri. In contrast, increased theta activity in the left cuneus was associated with slower reaction times across years of the study. PCG: precentral gyrus; STG: superior temporal gyrus: IPC: inferior parietal cortex; CUN: cuneus.

Table 1

Coordinates of significant cluster peaks for paired samples *t* test of time 2 versus time 1 oscillatory dynamics.

Oscillatory Band/Region	x	y	z
Theta			
R lateral prefrontal gyrus	41	−77	−13
R inferior occipital gyrus	35	56	28
Beta			
L superior temporal gyrus	−57	−2	−1
L inferior frontal gyrus	−51	31	−1
R parahippocampal gyrus	31	−9	−30

Note: Peak coordinates are in MNI standard coordinate space. There were no clusters that survived thresholding within the gamma window.